Particle Accelerators
1980, Vol. 10, pp. 107-123
0031-2460/80/1001-0107$4.50/0

PROPOSED METHOD FOR THE TRANSPORT OF IONS IN LINEAR ACCELERATORS UTILIZING ELECTRON NEUTRALIZATION†

STANLEY HUMPHRIES, Jr. and JAMES W. POUKEY

Sandia Laboratories, Albuquerque, New Mexico 87185 USA

(Received October 12, 1978; in final form March 26, 1979)

A geometry is proposed in which it may be possible to introduce electrons into ion beams within a linear-accelerator structure. In the configuration, electrons are controlled by solenoidal magnetic fields of moderate intensity; the electron flow guides the ion beam electrostatically, eliminating the need for direct magnetic focusing. Such systems may be capable of containing ion beams at levels up to the kiloampere range. Models are given for electron neutralization of ion beams over short time scales, the focusing properties and current transport limits for the electron-flow geometry, and the orbital stability of beams.

I. INTRODUCTION

The potential application of ion accelerators to inertial confinement fusion[1-4] has prompted consideration of methods of relaxing space-charge limitations to ion-beam transport. In accelerators with unneutralized beams, the most common approach has been to overcome space-charge repulsion by strong quadrupole magnetic lenses. Limits on beam current in this case have been discussed by Maschke.[5] In the present paper, methods are suggested for introducing electrons into the ion beam within an accelerator to produce almost complete cancellation of space-charge forces. Moderate magnetic fields limit the region accessible to electrons while preventing backflow. The control of the electron orbits results in the creation of strong electrostatic confining forces. In this sense, the electrons act as an amplifying intermediary so that the beam can be contained by magnetic fields much smaller than those needed to directly focus the ions. Such a system would have a considerable cost advantage over conventional focusing systems. A viable method of electrostatic transport is particularly attractive for heavy-ion accelerators.

The basis of electron neutralization on short time scales and the general concept of the neutralized linear accelerator are discussed in Section II. Section III introduces the method used to treat the transverse-focusing problem. Effects of applied magnetic fields, electrostatic confining fields, as well as space-charge repulsion in the accelerating gaps are included. The model is applied in Section IV to find beam-transport limits, in Section V to derive self-consistent transverse phase-space distributions, and in Section VI to investigate beam orbital stability. Practical considerations relating to the geometry are discussed in Section VII.

II. ELECTRONS IN LINEAR ION ACCELERATORS

Before considering the specific accelerator geometry, it is useful to present ideas on the electron neutralization of ion beams. The process in field-free regions over long time scales is a familiar phenomenon.[6] Here, ionization of background gas can act as an electron supply within the beam. The advent of high-intensity pulsed ion sources[7] has brought about consideration of the time-dependent neutralization problem. On nanosecond time scales, background ionization will be negligible for good vacuum. The simplest approach in this case is to provide sources of free electrons on the boundaries surrounding the vacuum region. These electrons can rush inward, attracted by the positive space charge at the approach of the pulsed ion beam or beam bunch. The time dependence of electron flow from boundaries into the ion beam volume has been considered for parallel injection in field-free regions[8] and for perpendicular injection in regions of magnetic fields transverse to the beam direction.[9] In general, it is found that electrons are attracted inward during the rise of the ion-beam density. The electron flux is limited mainly by space-charge constriction. If the source is not too far from the ion-

† This work was supported by the U.S. Department of Energy, under Contract AT(29-1)-789.

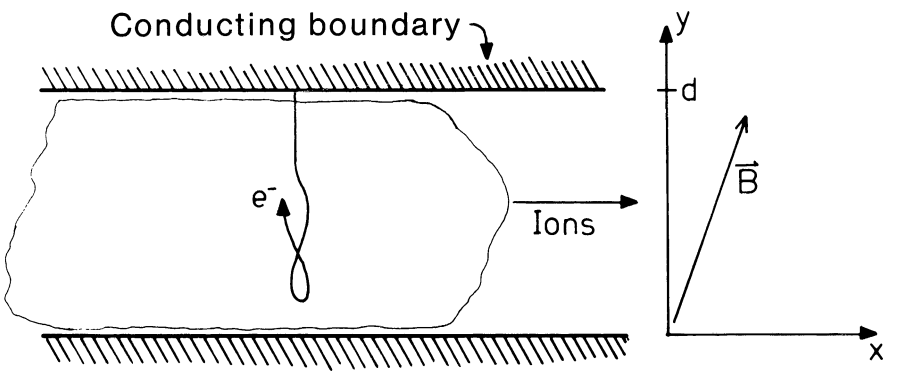

FIGURE 1 Transport of ions across a magnetic field with neutralization by electrons supplied from surrounding conducting boundaries.

beam boundary, the light electron mass allows high fluxes with relatively small residual space-charge potentials. Equilibrium calculations of the process in a geometry with one-dimensional symmetry[10] predict ineffective neutralization with a high central potential. On the other hand, in time-dependent cases with realistic geometry, the neutralizing electron velocity distribution can become randomized. In this case, electrons that have already entered the ion-beam volume have little effect on others entering from the source, so there is a continuous inward flux that eventually depresses the potential to zero.

With this type of electron flow, it is possible for ions to traverse magnetic fields strong enough to confine the electrons, while still maintaining space-charge neutralization, as shown in Fig. 1. If electrons have access to all field lines occupied by the beam, they can flow inward during the rise of the ion density and leave with the passage of the beam. This case has been studied with a time-dependent computer-simulation model.[11] The calculations confirm the electron space-charge flow limit and the importance of electron velocity relaxation. In the model, the boundaries (see Fig. 1) are assumed to supply electrons to fulfill the $E_y(0) = E_y(d) = 0$ condition, the uniform ion density rises linearly with time and then becomes constant, and the effects of electron relaxation are introduced into the one-dimensional system by canting the magnetic fields at a small angle with respect to the boundaries. Typical calculations treat a beam rising to $n_i = 10^{-12}$ cm^{-3} in 0.5 nsec, corresponding to a current density of the order of kA/cm^2 and an unneutralized central potential of 250 kV. If the electrons are introduced, but the system is symmetric (magnetic field lines normal to the wall), the central potential reaches a steady-state value of 40 kV. If the field lines are canted so that electrons develop velocity components transverse to the field, the space-charge potential is reduced to less than 1 per cent of the unneutralized value within 1 nsec, and continues to decrease. The theoretical models[8,9,11] as well as experiments on intense pulsed ion beams in transverse magnetic fields[12,13] indicate that a good first approximation for the neutralization process of low-β ion beams is to assume that beams (or bunches in conventional accelerators) with rise times on the order of a few nanoseconds or more are completely neutralized in regions accessible to electrons from boundary sources.

The system of Fig. 2 is proposed as a method of utilizing rapid electron neutralization in the drift tubes of a linear ion accelerator. The major differences from a conventional structure are the presence of solenoidal magnetic fields, which make cusps at the accelerating gaps and electron sources at the tube entrances. The magnetic field must prevent electron backflow in the accelerating gaps, which is important for two reasons. First, the backflow of electrons could constitute a power drain and second, the loss of electrons from the drift tubes would prevent the build-up of an adequate density for neutralization. The major disadvantage of the simple cusp fields compared to more complex magnetic field geometries[9] is the opening on the axis. If attempts were made to neutralize a cylindrical ion beam in the geometry of Fig. 2, there would be a large electron leakage. On the other hand, if the ion beam were annular in cross section, electrons could be prevented from reaching the axis, eliminating the problem. This can be accomplished by the selective production of neutralizing electrons.

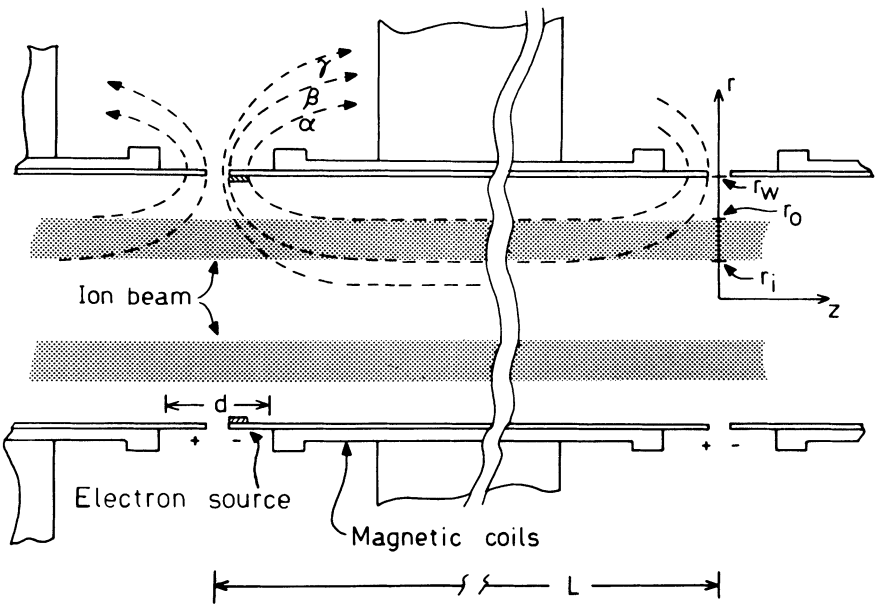

FIGURE 2 Geometry for introducing neutralizing electrons into the drift tubes of a linear accelerator.

Referring to Fig. 2, it is assumed that the walls of the drift tube contain electron sources[14] on their inner surfaces at the entrances. These electrons can flow along field lines external to line β. Lines internal to this line (line γ, for instance) curve back on the outside and connect to electrically unstressed portions of the drift-tube support structure. Because of the low electric fields and long vacuum paths, electrons are not supplied on internal lines, even under very high gap-field stress. This has been verified experimentally in a similar geometry.[15] Ions attempting to enter the region $r < r_i$ are unneutralized and build up a repulsive positive space charge. Thus, the inner boundary of the annular ion beam can be maintained by electrostatic repulsion. Containment on the outer boundary can be either magnetic (note that the magnetic field is equivalent to a series of solenoidal lenses) or electrostatic. The electrostatic option results if electron production is inhibited on parts of the drift-tube inner surface connecting to field lines external to line α. In this case, neutralizing electrons controlled by relatively weak magnetic fields define an annular region. Ions are prevented from leaving this electron-flow annulus by their own space-charge forces. The situation is unusual in that the ions can be contained by space-charge forces, rather than dispersed. (In Section III, details of the formation of electrostatic sheaths will be discussed.) The restoring forces that act on the transverse beam dynamics are highly nonlinear. In this paper the term focusing will be reserved for linear elements, while the term containment will be applied to the nonlinear ion-beam control of the system of Fig. 2. It will be shown that the nonlinear containment system does not preclude the production of beams of good quality which can then be focused to a target by linear elements.[16]

As has been mentioned, the cusped magnetic fields not only channel electrons along the proper annulus, but also prevent electron backflow in the accelerating gaps. This allows high field stresses to be applied in the gap.[17] The available longitudinal field gradient can be concentrated in a small fraction of the accelerator length. This is important because the ion beam will be unneutralized in the accelerating gaps, so the relative amount of time it spends there should be minimized. In Fig. 2, if the gap has an average width d and the drift tube has length L, then the neutralization of the beam in the drift tube reduces the effects of space charge roughly a factor of (d/L). The minimum magnetic field necessary to prevent electron backflow is called the critical insulating field, B^*. If δ is the spacing of the drift tubes at the point of maximum electric-field stress, then B^* is given approximately by

$$B^* = (2\, eV_0/r_e)^{1/2}\,(1 + eV_0/2m_ec^2)^{1/2}/\delta, \quad (1)$$

where V_0 is the applied voltage and r_e is the classical

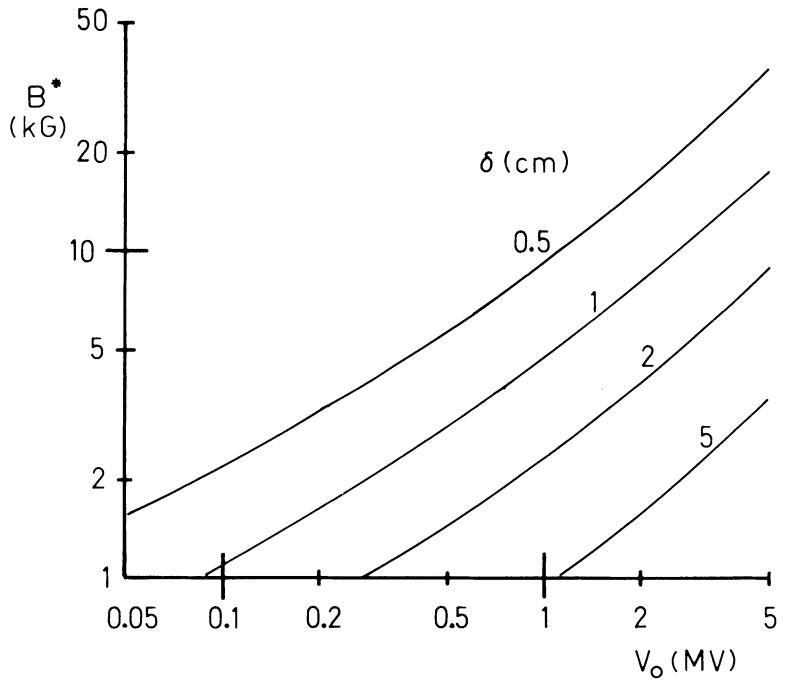

FIGURE 3 Critical insulating magnetic field in terms of gap spacing and applied potential (parallel plate approximation).

electron radius. A plot of B^* versus V_0 for various values of δ is given in Fig. 3. It can be seen that modest magnetic fields will provide insulation of gaps even into the megavolt range.

III. EFFECTIVE TRANSVERSE CONFINEMENT POTENTIALS

The exact treatment of ion orbits in the neutralized system, including nonlinear confinement effects from the electrostatic sheaths and the self-consistent inclusion of beam space charge in the accelerating gaps, is a difficult problem. A useful approximation that provides a straightforward and general description of beam dynamics is to average the confinement forces over a number of drift tubes and accelerating gaps. The average forces can then be integrated to give effective confinement potential wells. In this way, the various factors entering the problem can be handled separately and then added to give a total potential. In addition, the changing parallel velocity of the ions does not enter into the problem except to determine certain adiabatically changing parameters such as beam density. Given the potentials, self-consistent beam distributions can easily be calculated. The validity of the approximation depends on two conditons: 1) the transverse oscillation frequency of the ions is small compared with the frequency of traversing gaps and 2) the periodic application of confining forces does not couple to the transverse oscillations to produce an orbital instability. The verification of these conditions will be deferred to Sections IV and VI.

As an example of the method, the magnetic forces acting on the ions from the applied solenoidal fields will first be considered. It is assumed that $d \ll L$, and that orbits through the lens array make small angles with the axis. In other words, it is sufficient to characterize the radial position of an ion in a particular drift tube or gap by an average r; this is equivalent to condition 1 above. By conservation of angular momentum, the component of azimuthal velocity in phase with the alternating direction of the solenoidal field (which gives a net radial deflection when averaged over many drift tubes) is $v_\theta = \pm eBr/2\ m_i c$, where B is the solenoidal field within the drift tube. The net radial force is then $F_r = -e^2B^2r/4\ m_i c^2$. This is the $v \times B$ force minus the centrifugal force, and is always directed inward. It acts almost continuously, since the ions spend a small fraction of their time in the acceleration gaps,

where the field is radial. The effective magnetic potential is then

$$U_m = -\int_0^r F_r\, dr = e^2B^2r^2/8\, m_ic^2 \text{ (ergs)}. \quad (2)$$

The effective potential well is quadratic, as expected, because solenoidal magnetic lenses are linear focusing devices in the paraxial approximation. Note that there is no dependence on the longitudinal velocity in Eq. (2), so the treatment of transverse orbits in this potential is independent of the acceleration process.

In a similar way, the formation of an electrostatic sheath at $r = r_i$, as the transverse energy of the ions causes them to penetrate the region forbidden to electrons, can be considered. An exact sheath solution would depend on the specific ion-energy distribution. Such a solution is not imperative, since it is generally true that the sheath will be thin compared with the beam annular thickness. In calculating ion orbits, it can be regarded as a reflecting surface. To estimate the sheath dimension, it is assumed that there is a uniform beam density n_i at r_i which is shifted inward a distance $\Delta\rho$ as shown in Fig. 4(a). At the same time, extra

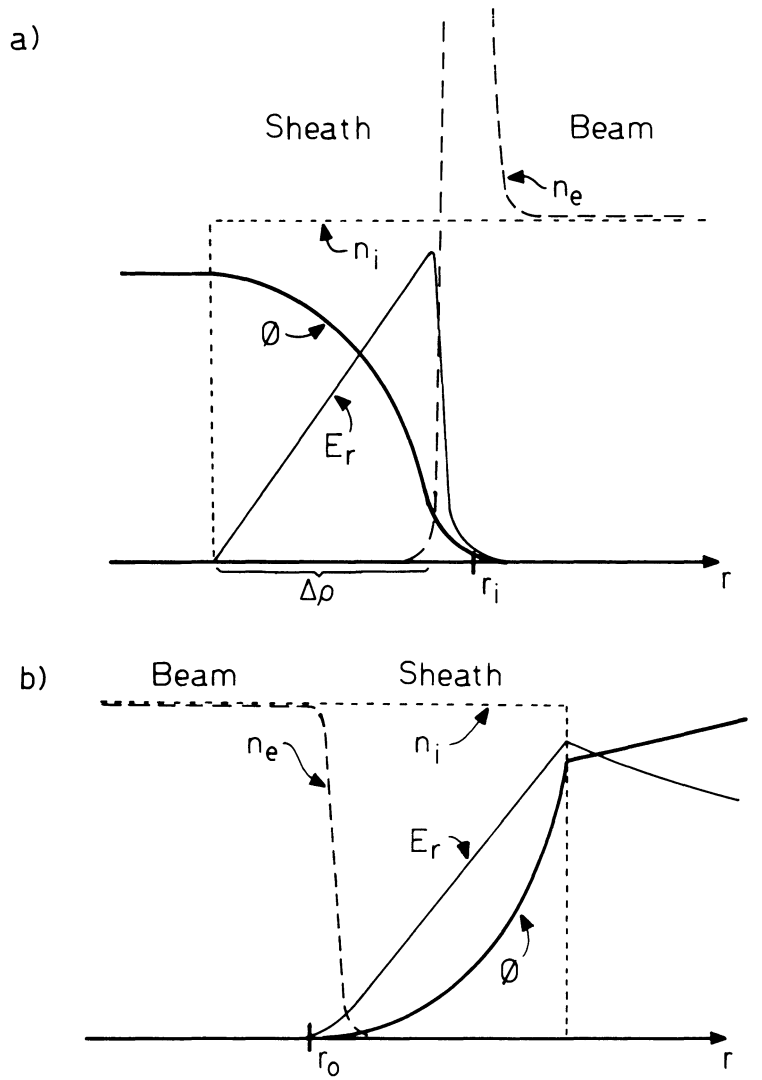

FIGURE 4 Electrostatic sheath formation at edges of electron annulus. a) Inner boundary. b) Outer boundary.

electrons have been drawn out on the field-line β to make $E_r = 0$ within the beam volume. It will be shown in Section IV that these electrons are confined closely to the field line compared to the sheath thickness. With this condition, typical curves for the radial electric field and electrostatic potential are shown in Fig. 4(a). The height of the electrostatic potential is approximately

$$\phi_{\max} \cong 2\,\pi e n_i\,\Delta\rho^2. \tag{3}$$

In terms of the effective potential model, $U_e(\max) = e\phi_{\max}$. The height of the sheath potential rises to reflect all ions, so that $U_e(\max) \sim E_{B\perp}$, where $E_{B\perp}$ is the transverse beam energy, determined by either the initial injection conditions or by space-charge effects in the accelerating gaps. For the case of an electrostatic sheath on the outer boundary of the beam ($r = r_0$ in Fig. 2), similar considerations apply although the electron behavior differs somewhat. The ions are shifted to slightly larger radii, decreasing the average ion density in the beam. In order to preserve an equipotential along field lines, electrons flow inward to match this lowered density. This gives zero net charge for $r \leq r_0$, and a net positive charge outside r_0. The external sheath is illustrated in Fig. 4(b).

In the case of electron emission on all field lines connecting to the inner drift-tube wall, there will be an electrostatic sheath at $r = r_i$ only, and the external confinement is magnetic. Adding the two effects gives the effective potential well shown in Fig. 5(a), of the form

$$U_T = (e^2B^2/8\,m_ic^2)\,(r^2 - 2\,r_i^2 + r_0^2),\ r < r_i \tag{4}$$
$$U_T = (e^2B^2/8\,m_ic^2)\,(r^2 - r_i^2),\ r > r_i.$$

The sheath has been assumed to be thin, and U_T taken as 0 at r_i. The total depth of the well (and hence r_0) is determined by the transverse beam energy. Note that the restoring forces are highly nonlinear and thus there is no unique transverse oscillation frequency. For a given maximum radius (r_w), the magnetic-field energy density must be increased in proportion to the ion mass in order to confine beams having the same transverse energy. Thus for heavier ions magnetic confinement using solenoidal lenses becomes impractical. A better option is to suppress electron emission along field lines having $r > r_0$ in the solenoid to produce an electrostatic sheath at $r = r_0$. The behavior of the effective potential in this case is shown in Fig. 5(b). The height of the sheath potential rises to match the beam transverse energy,

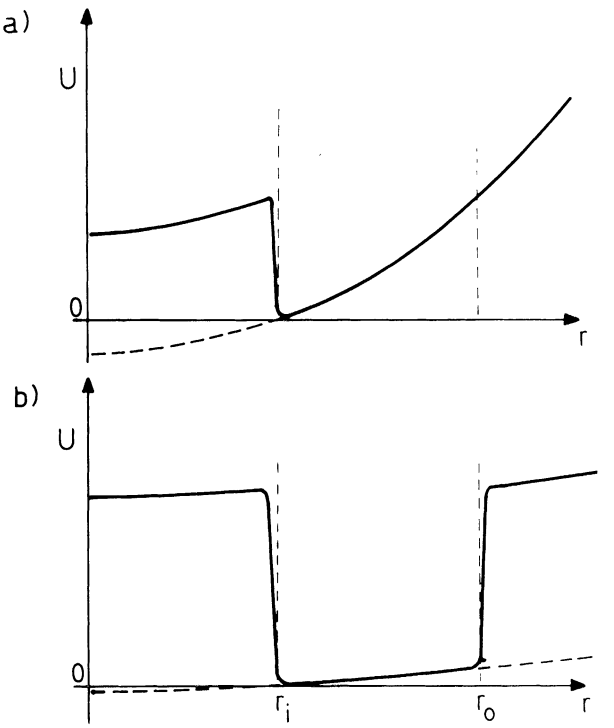

FIGURE 5 Forms of effective potential wells with magnetic and electrostatic sheath effects. a) Strong magnetic effects with complete neutralization for $r > r_i$. b) Weak magnetic effects with both external and internal sheaths.

with no dependence on ion mass as long as there is sufficient ion density (see Section IV). For heavier ions and moderate magnetic fields, the contribution of magnetic fields to the effective potential can become small. In this case, the radial potential well approaches a square well and the main purpose of the magnetic field is to channel electrons along the appropriate annulus.

Because of the irregular geometry of the accelerating gaps, it is difficult to treat this region exactly. Instead, general scaling laws will be derived to gain a rough estimate of residual space-charge effects. As the ion beam proceeds towards an accelerating gap, at some point the accompanying electrons will exit along magnetic-field lines. This occurs at the position where the repulsion of electrons by the applied field in the gap exceeds the attraction of the positive-ion space charge. (A discussion of this effect is given in Ref. 9.) The ions will thus be unneutralized until they cross the gap to pick up electrons from the next drift tube. The unneutralized portion of the beam's travel is characterized by an effective gap distance

d. If it is assumed that the transverse components of the accelerating electric field have positive and negative components that approximately cancel as the beam traverses the gap, then the increase in beam transverse energy is caused mainly by space-charge repulsion. The space-charge distribution of Fig. 6 can be used to estimate this process. The magnetic field flux surfaces that define electron flow upstream and downstream can be taken as conductors. In the case of a thin annulus with $\Delta r \ll r_i$, $\Delta r \ll d$, and uniform ion density, the conducting boundaries can be neglected. The space-charge potential across the minor dimension approximately obeys the one-dimensional equation $d^2\phi/d\rho^2 = 4\pi en_i$. The quantity ϕ is given by $\phi = \phi_{\max} - 4\pi en_i\rho^2/2$, where $\phi_{\max} = \pi en_i\Delta r^2/2$. When $\Delta r \sim d$ (a thin accelerating gap), the conducting boundaries are important, shorting out space-charge contributions to the potential except within a distance of the order of d from the edges of the beam. In this case, the potential averaged across the gap has a maximum of $\phi_{\max} \sim \pi en_i d^2/2$. In the typical case (see Fig. 2), d will be of the order of Δr. If this is true, a geometric scaling factor α of the order of unity can be introduced so that the average maximum space charge in an accelerating gap can be written

$$\phi_{\max} = \alpha\pi en_i d^2/2. \tag{5}$$

The scaling factor accounts for boundary conditions and the finite length of the unneutralized part of the beam. The depth of the space-charge contribution to the effective potential is then

$$U_{sc}\,(\max) = (\alpha\pi/2)\, e^2 n_i d^2\, (d/L). \tag{6}$$

Note the (d/L) factor. In the average model, there is no dependence on longitudinal velocity. This comes about because the space-charge forces act over a time interval (d/v_z) with frequency $f_z = (v_z/L)$, so that the v_z factor cancels.

A typical total potential well is shown in Fig. 7. Some qualitative observations can be made based on a general knowledge of particle oscillations in potential wells. 1) When space charge is negligible and magnetic confinement is used, the depth of the potential well must be on the order of the beam transverse energy, which will probably be determined by injection conditions and the confinement properties of the magnetic lenses. 2) In the case of predominantly electrostatic focusing, the beam boundaries are determined by the magnetic-field geometry and the location of electron sources. The height of the electrostatic sheath potential rises to reflect the ions. 3) When gap space charge is significant, the periodic repulsive forces will increase the beam transverse energy above the injection energy. After many gaps, the beam will fill in the effective potential well and acquire an equilibrium transverse energy of $E_{B\perp} \sim E_{B\perp}$ (Injection) + U_{sc} (max). These considerations will be applied in Section IV to

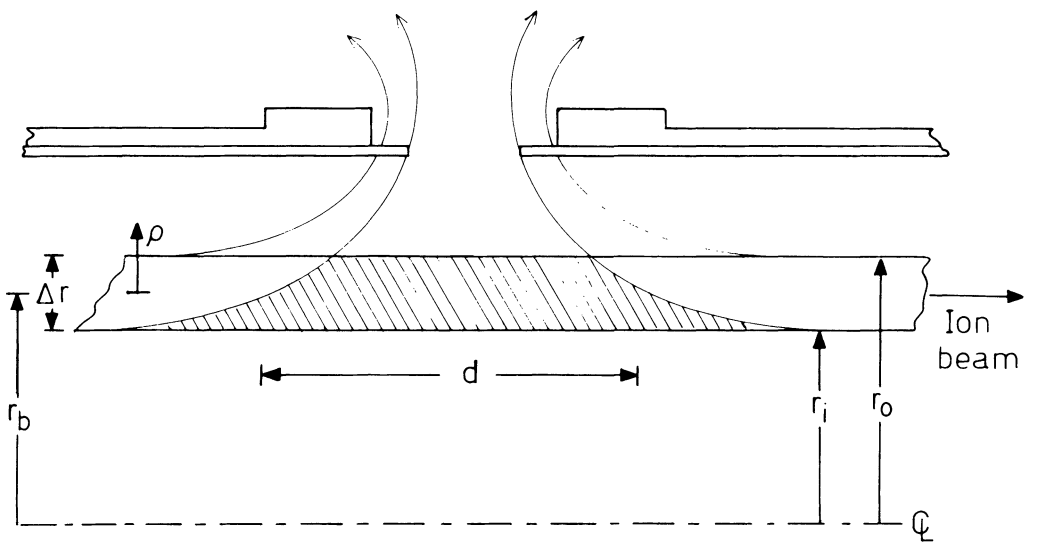

FIGURE 6 Geometric parameters relating to ion beam space-charge effects in an accelerating gap.

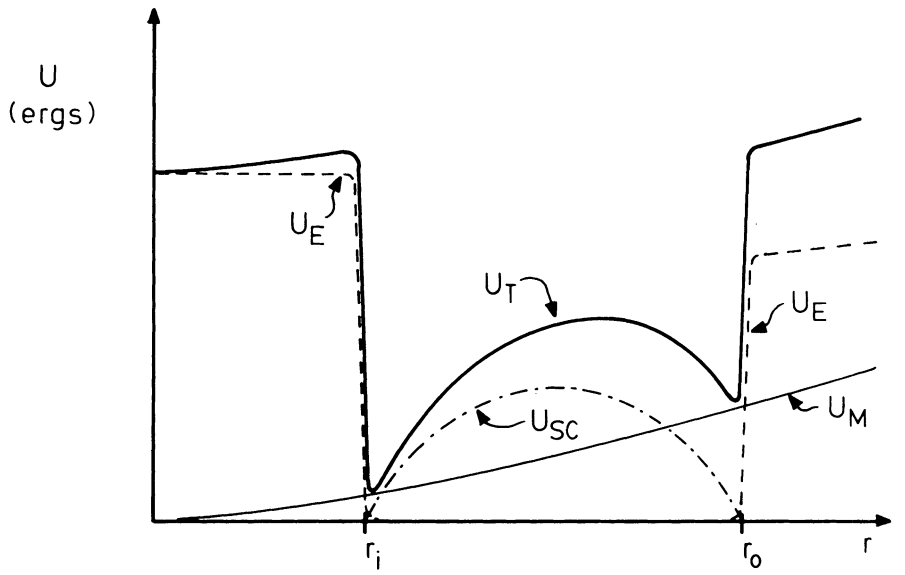

FIGURE 7 Total effective potential confining well (U_T), with contributions from magnetic fields (U_M), electrostatic sheaths (U_E) and accelerating gap space-charge effects (U_{sc}).

estimate beam transport limits and other parameters.

IV. BEAM TRANSPORT LIMITS

Before considering factors that limit the transport of current in neutralized linear accelerators, typical values for a number of relevant physical parameters will be calculated. The first example is the sheath thickness $\Delta\rho$ determined by Eq. (3). Fig. 8 gives a plot of ion-beam density as a function of current density and energy per nucleon. Typical beam densities might range between $n_i = 10^{10}$ cm^{-3} and 10^{12} cm^{-3}. The sheath thickness is given as $\Delta\rho = (E_{B\perp}/2\,\pi e^2 n_i)^{1/2}$, where $E_{B\perp}$ is the transverse beam energy. The quantity $E_{B\perp}$ is determined by either the initial injection conditions or by space-charge repulsion in the accelerating gaps, as discussed in Section III. In the first case, $E_{B\perp}$ is given by $E_{B\perp} \cong E_{BO}\Delta\theta_0^2$, where E_{BO} is the longitudinal energy at injection and $\Delta\theta_0$ is the initial divergence. For example, with a 1-MeV injector and a half-angle of divergence of 2°, the perpendicular energy is 1200 eV. With this figure and a minimum density of 10^{10} cm^{-3}, the sheath thickness is about 1 mm, small compared to beam dimensions that would typically be a few centimeters. For the case of beam transverse energy determined by space-charge repulsion, the transverse energy can be taken as $E_{B\perp} \sim U_{sc}(\max)$, given by Eq. (6). When this is substituted into Eq. (3), it is found that

$$\Delta\rho \cong \tfrac{1}{2}\, d\, (d/L)^{1/2}. \tag{7}$$

Since in practical cases $d \ll L$ and $d \lesssim r_b$, the sheath will be thin compared to the beam dimensions.

The magnetic fields that control the electron motion must satisfy two requirements. First, they must provide sufficient magnetic insulation of the accelerating gaps to prevent losses of electrons from the drift tubes. As shown in Fig. 3, fields on the order of a few kilogauss should suffice. Second, the fields must be strong enough in the drift tubes to confine electrons to less than an electrostatic sheath thickness in order for the model of a sharp boundary to be valid. In the case of a uniform electric field perpendicular to a magnetic field, a single-particle orbit estimate shows that a zero-energy electron entering the electric field region is confined within a distance

$$\delta_B = 2\, r_{ge} = 2\, m_e c v_d/eB = 2\, m_e c(cE/B)/eB, \tag{8}$$

by the magnetic field. Here v_d is the $E \times B$ drift velocity. The condition for the magnetic excursion δ_B to equal the sheath thickness $\Delta\rho$ will be derived. In this case, the electric field can be approximated as $\phi_{\max}/\delta_B$, using $\phi_{\max}$ from Eq. (3). By substitution, it is found that $\delta_B \leq \Delta\rho$ when

$$B^2/8\,\pi \geq n_i m_e c^2/4. \tag{9}$$

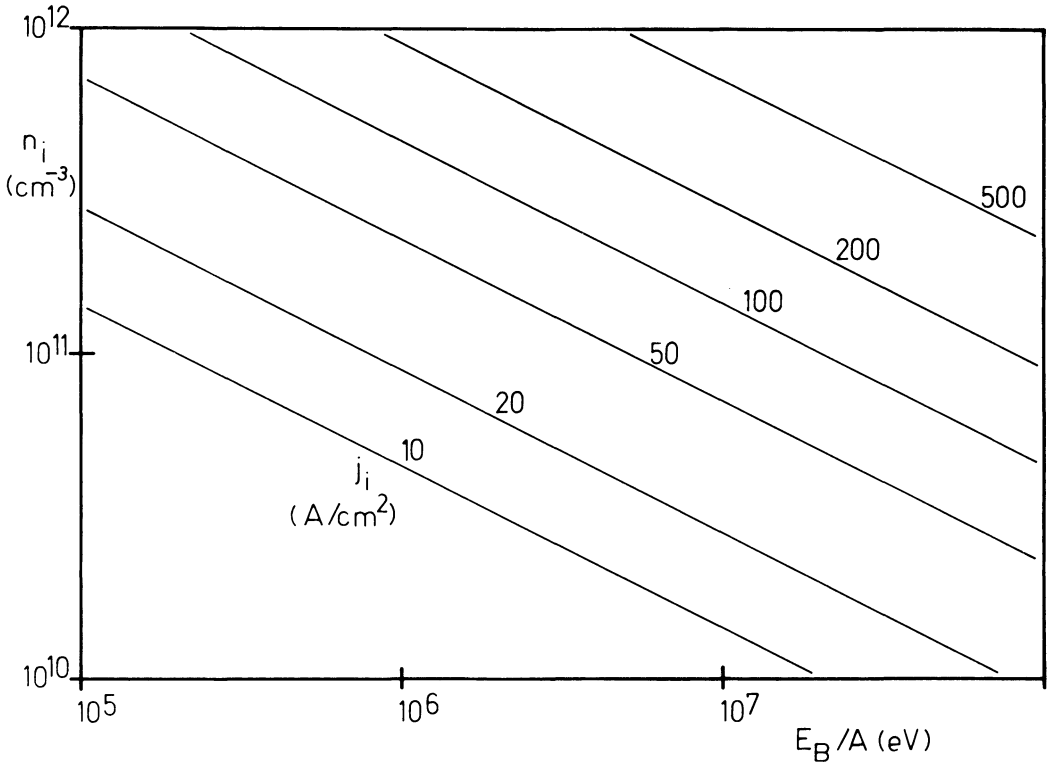

FIGURE 8 Ion beam density as a function of current density (j_i) and energy per nucleon (E_B/A).

As an example, when $n_i = 10^{12}$ cm^{-3}, then B must be greater than 2.3 kG to satisfy Eq. (9). Thus fields of a few kilogauss can confine electrons in the drift tubes even for high ion densities.

In systems with magnetic confinement, there is a limit to the transverse beam energy that can be handled. If the beam energy results mainly from the injection process, the limit can be written

$$E_{BO}\Delta\theta_0^2 < (e^2B^2/8\ m_ic^2)\ r_w^2, \qquad (10)$$

where r_w is the radius of the physical boundary of the drift tube. For example, if $r_w = 10$ cm, $B_z = 10$ kG and $E_{BO} = 1$ MeV, then for proton transport the initial divergence must be less than 19°. For the same parameters using N^+, the divergence must be less than 5°. Thus for light and intermediate ions the initial perpendicular energy does not present much problem. A more stringent constraint on magnetic confinement using solenoidal lenses arises from the effects of gap space charge. A beam limit can be estimated by setting U_m (max) ($= e^2B^2r_w^2/8m_ic^2$) equal to U_{sc} (max) [see Eq. (6)]. This gives the approximate condition

$$B^2/8\ \pi > \tfrac{1}{2}\alpha n_i m_i c^2\ (d/L)\ (d/r_w)^2. \qquad (11)$$

B is plotted in Fig. 9 as a function of αn_i for various ion species. With protons, magnetic confinement can be quite effective. Beam densities up to 10^{12} cm^{-3} can be accomodated with fields on the order of 10 kG. For example, with $(d/L) = 0.05$, $\alpha = 1$, and $(d/r_w) = 0.2$, then $B > 6.1$ kG. This rises to 23 kG for N^+.

In systems with electrostatic confinement, extremely high currents can be transported if there is no limit on beam divergence. Specifying a maximum beam (or transverse energy) sets an upper limit on current, as explained in Section III. For instance, it might be necessary to produce a focal spot of radius Δx a distance D from a final focusing lens. In this case, the final beam divergence must be $\Delta\theta_f \lesssim \Delta x/D$. The transverse beam energy is $E_{Bf}\Delta\theta_f^2$, where E_{Bf} is the final longitudinal energy. This quantity must be of the order of U_{sc} (max). In order to relate this to a current limit, it is useful to rewrite U_{sc} (max) as

$$U_{sc}\ (\text{max}) = (1.6 \times 10^5)\ \alpha I(d/L)\ (d/r_b)/(E_B/A)^{1/2},$$

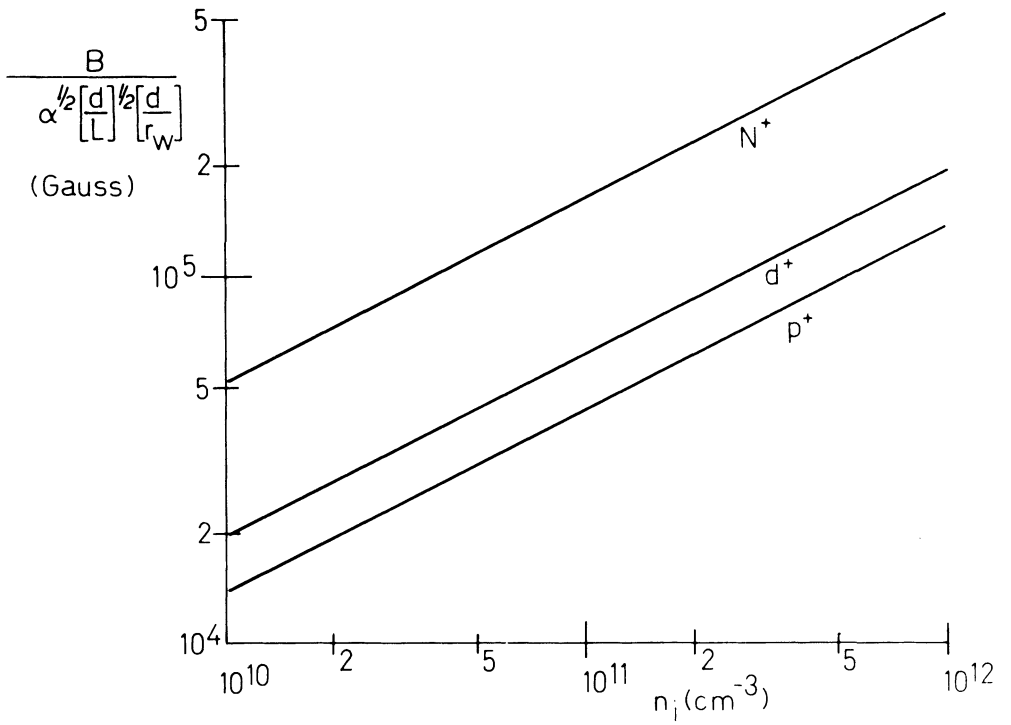

FIGURE 9 Magnetic field requirements for the magnetic confinement of space-charge limited beams in terms of beam density.

where U_{sc} (max) and E_B are in eV and I in amps. The total beam current has been taken as $I = en_i v_z\ (2\ \pi r_b \Delta r)$. The limit on beam current set by space-charge effects and a divergence requirement is then

$$I < (6.2 \times 10^{-6})\, E_{Bf} \Delta\theta_f^2\, (E_B/A)^{1/2}\, (L/d)\, (r_b/d)/\alpha. \tag{12}$$

The following example is appropriate to a fusion application.[4] If it is necessary to focus on a 0.5-cm radius pellet from a distance of 4 m, then the final divergence angle must be on the order of 1.25×10^{-3} radians. If E_{Bf} is 1 GeV, (E_B/A) at the point of interest is 10 MeV per nucleon, $(d/L) = 0.05$ and $(d/r_b) = 0.25$, then the current limit would be about 2.5 kA. In theory, it is possible to transport large currents through nonlinear transport elements while still maintaining good beam quality.

The final matter to be considered is the validity of the effective potential model with respect to the magnitude of the transverse-oscillation frequency compared with the frequency of traversing gaps. The gap traversal frequency, f_z, characterizes the time scale of variations in the transverse forces and is given by $f_z = v_z/L$. In the nonlinear potential wells considered, there is no unique radial-oscillation frequency, but an average can be taken as $f_r = v_r/2\Delta r$. In terms of the local divergence angle, $\Delta\theta = v_r/v_z$, the condition $f_z \gg f_r$ holds if

$$\Delta\theta \ll (2\ \Delta r/L). \tag{13}$$

As an example, consider $\Delta r = 2.5$ cm and $L = 100$ cm. The $\Delta\theta$ should be less than 3°. This could be satisfied at injection and almost certainly is satisfied in latter stages of the accelerator where the divergence has been reduced by longitudinal acceleration.

V. SELF-CONSISTENT TRANSVERSE BEAM DISTRIBUTIONS

An important problem related to the nonlinear transport elements of the neutralized linear-accelerator geometry is the existence and choice of equilibrium transverse phase-space distributions. If the beam has such an equilibrium, it will propagate without change in cross section. Calculated dis-

tributions can indicate the optimum injection conditions to minimize beam oscillations. As has been pointed out, the longitudinal velocity does not enter into the transverse problem directly, but rather determines parameters such as the local value of space-charge fields, particle mass in the case of relativistic particles, and so forth. If these parameters vary slowly compared with the transverse oscillation frequency, the beam transverse distribution will change adiabatically and proceed through a series of approximate equilibria.

Using the effective-potential model, it is possible to compute steady-state beam distributions even in the case where the beam determines the potential variation. Given the externally applied components of the effective potential and a law to relate potential to the beam density, there is a straightforward method for computing the self-consistent density distribution.[18] This is most easily done in the case of particles oscillating in a one-dimensional potential well that increases monotonically from a minimum point. The velocity distribution will vary as a function of position. A more convenient quantity is the flux distribution measured at the point of minimum potential. The flux distribution F is defined as

$$F(v_{\rho 0})dv_{\rho 0} = fv_{\rho 0}, \tag{14}$$

where f is the fraction of total number of particles having $v_{\rho 0}$ in $dv_{\rho 0}$ at ρ_0 and $U_T(\rho_0) = 0$. Considering one group of particles, if the distribution is in a steady state, then the flux of these at any point must be equal either to the flux at ρ_0 (if the particle is energetic enough to reach the point) or to zero if the point lies beyond the particles' turning point. Thus these particles make a contribution to the local density of

$$dn(\rho) = n_0 F(v_{\rho 0})dv_{\rho 0}/v_\rho \text{ if } U_T(\rho) - m_i v_{\rho 0}^2/2, \tag{15}$$

or $$dn(\rho) = 0 \text{ if } U_T(\rho) > m_i v_{\rho 0}^2/2,$$

where $n_0 = n(\rho_0)$. Noting that $v_\rho = (v_{\rho 0}^2 - 2\,U_T/m_i)^{1/2}$, we can write the total density as a function of U_T, as

$$\frac{n(U)_T}{n_0} = \int_{(2\,U_T/m_i)^{1/2}}^{v_{\rho 0}\,(\max)} \frac{F(v_{\rho 0})\,dv_{\rho 0}}{(v_{\rho 0}^2 - 2\,U_T/m_i)^{1/2}}. \tag{16}$$

The integration is taken over all particles that can reach the point where the potential is equal to U_T. Given $n(U_T)$ combined with a functional relationship to give U_T in terms of $n(\rho)$, the problem can be solved self-consistently.

Two examples of this calculation will be treated: 1) the distribution in a magnetic focusing system with negligible space-charge effects and 2) the distribution with negligible magnetic confinement with the inclusion of space-charge effects. A thin-annulus approximation will be used so that variations are one-dimensional in ρ. If this were not the case, a $1/\rho$ term would have to be introduced into Eq. (16), and the density could not be expressed solely in terms of U_T. The choice of flux distribution is somewhat arbitrary, so a distribution will be used that represents a randomized collection of particles and gives a closed-form solution to Eq. (16). If $f = 3\,[1 - (v_\rho/v_{\rho 0}\,(\max)]^2 dv_{\rho 0}\,(\max)$ and $\frac{1}{2}\,m_i v_{\rho 0}\,(\max) = U\,(\max)$, then the density is found to be

$$\frac{n(U_T)}{n_0} = \left(1 - \frac{U_T}{U_{T\max}}\right)^{3/2}. \tag{17}$$

For the case of magnetic confinement with a sharp electrostatic inner boundary, the potential can be written as in Eq. (4). This can be combined with the distribution of Eq. (17) to yield the spatial density plotted in Fig. 10.

With space-charge effects included, the ion density determines the repulsive contribution to the effective potential (see Fig. 7). If magnetic effects on the ion orbits are small, the applied effective potential will be approximately a square well, as in Fig. 5(b). The height of the well is determined by the total beam transverse energy, and for non-ideal injection will generally be higher than $U_{sc}\,(\max)$. In the case of a thin annular beam ($d \gg \Delta r$), the space-charge part of the effective potential will be related to the density approximately through Poisson's equation, $d^2U_{sc}/d\rho^2 = -A\,[n(U_T)/n_0]$, where A is a parameter to be adjusted to meet the boundary conditions. In the case of the square well, there are no applied-potential variations across the region occupied by the beam, so in this region it is possible to write for U_T

$$\frac{d^2\,[U_T/U_T\,(\max)]}{d\rho^2} = -\frac{A}{(\Delta r/2)^2}\left[1 - \frac{U_T}{U_T\,(\max)}\right]^{3/2}. \tag{18}$$

For various choices of $U_T\,(\rho = 0)/U_T\,(\max)$, this equation can be solved with A adjusted to satisfy the boundary conditions $U_T(\rho = 0) = U_{sc}\,(\max)$ and $dU_T/d\rho = 0$ at $\rho = 0$, and $U_T = 0$ at $\rho = \pm\Delta r/2$. In this case, there are two points of minimum potential. But since the well is symmetric, particles

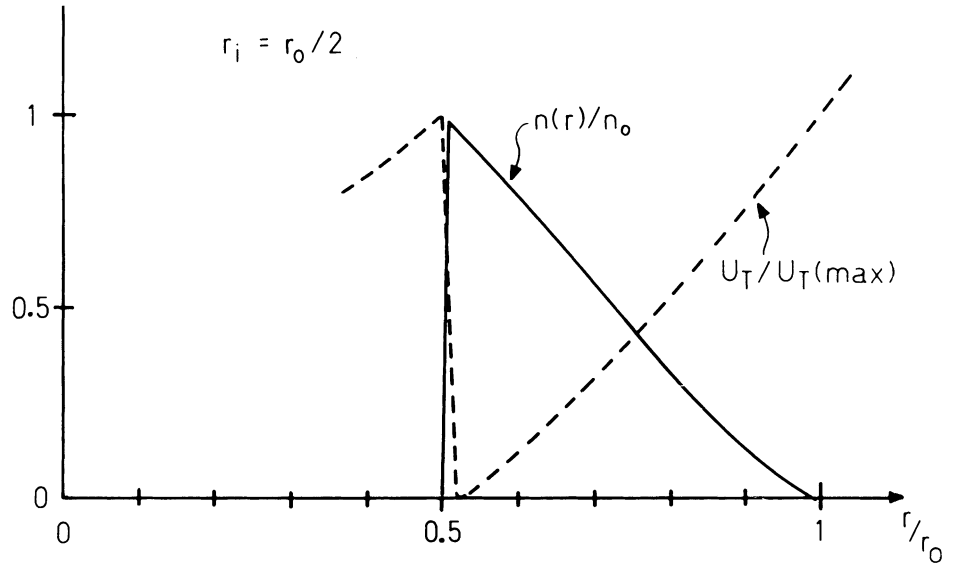

FIGURE 10 Example of self-consistent density distribution for ions confined in a magnetic well with negligible space-charge effects.

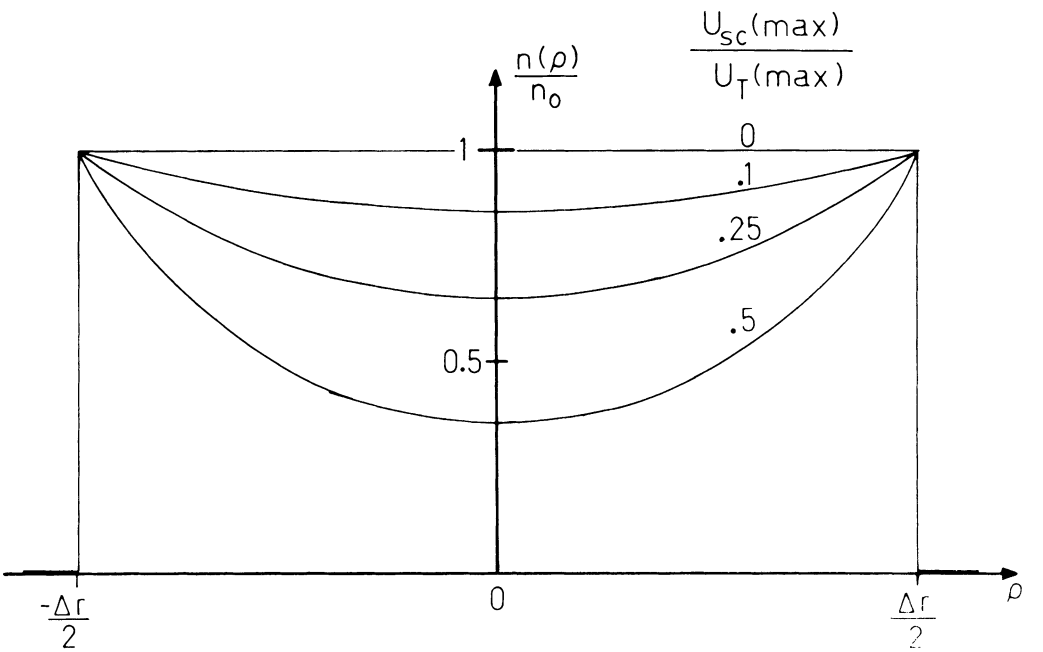

FIGURE 11 Self-consistent density distributions for electrostatically confined ions with gap space-charge effects included. U_{sc} (max)/U_T (max) is the ratio of the depth of the effective space-charge potential well to the total transverse beam energy.

crossing the midplane can be considered to be reflected, and hence it is sufficient to deal with one class of particles occupying half the well. In the general case of non-symmetric wells with more than one minima, the problem becomes more complex because there may be a number of different groups of trapped and untrapped particles relative to the various minima. Figure 11 shows self-consistent

tranverse-density variations for the square well with space-charge effects. As the space-charge potential U_{sc} (max) rises with respect to the total beam energy, the density profile is hollowed. An alternative approach to the problem with application to the choice of injection parameters would be to assume a beam profile (uniform, for instance), which would determine an effective potential. Then, the above process could be inverted to find the appropriate beam-velocity distribution that should be approximated at injection.

The two examples treated could be approached analytically because of the particularly simple geometries. Real cases will be complicated by finite-width annuli, magnetic-field effects, and electron-flow dynamics on each side of the accelerating gap. Presently, such cases with realistic geometries are being studied by numerical-simulation methods.

VI. TRANSVERSE ION ORBITS

In this section, the validity of the effective potential model will be investigated by the numerical computation of ion orbits. In particular, it will be shown that as f_z becomes much greater than f_r, the ion orbits will approach those predicted by a continuous effective potential, even though the force may be applied periodically for a brief instant (as in the case of the gap space-charge forces). It will also be seen in the model chosen that because of the high nonlinearity of the effective potential wells, there is little unstable coupling of the periodically applied forces to the transverse oscillations.

In order to simplify the calculations, the applied potential will be taken in the form of a square well of width Δr [see Fig. 5(b)]. Since the ions sample this well for the majority of the time, periodic variations in the applied fields will be neglected. Such variations appear mainly in the accelerating-gap space-charge forces, which are assumed to act instantaneously with a frequency f_z. The effect of the space-charge forces in the paraxial approximation is to give an ion a transverse velocity deflection δv_ρ as it crosses the gap of width d; the velocity deflection will be a function of position [see Fig. 12(a)]. In order to relate this to the physical parameters already introduced, the electrostatic potential in the gap (averaged over the length d) is approximated by the expression

$$\phi_{sc}(\rho) \cong \phi_{sc}\ (\max)\ [1 - (2\ \rho/\Delta r)^2].$$

The average transverse force on an ion will then be $\bar{F} = -[(d/d\rho)\,(e\phi)]$. The velocity deflection is given by $\delta v_\rho = (F/m_i)\ (d/v_z)$ and it can be written as

$$\frac{\delta v_\rho(\rho)}{v_z} = \left[\frac{\delta v_0}{v_z}\ \frac{2\rho}{\Delta r}\right], \tag{19}$$

where $\delta v_0/v_z = (2\ L/\Delta r)\ U_{sc}\ (\max)/(m_i v_z^2/2)$. Here $e\phi_{sc}\ (\max)$ has been expressed as $U_{sc}\ (\max)\ (L/d)$ in order to relate these calculations to the effective-potential model. A typical ion orbit is shown in Fig. 12(a). The main information of interest is the behavior of the radial velocity v_ρ with time. The positions ρ and z are not important except to calculate the velocity deflections. The problem can be simplified by neglecting the reflections from the applied potential. In other words, an equivalent problem results from removing the reflecting boundaries and lining up an infinite sequence of gap potentials in ρ with period Δr. The transverse position variable is defined as $x = v_\rho^* dt$, where v_ρ^* is the radial velocity neglecting reflections at the boundary (although there may be reflections at the midplane). The form of the velocity changes is shown in Fig. 12(b). The velocity is modified every time interval $\Delta t_z = (L/v_z)$ according to the velocity change at the position x. A uniform v_z is assumed. With a changing v_z, the transverse-velocity problem is unchanged in the effective-potential limit ($f_r/f_z \ll 1$) since the deflection of Eq. (19) scales as $1/v_z$ and the number of deflections per time interval is proportional to v_z.

If x_n and $v_{\rho n}$ are the transverse position and velocity just before the nth accelerating gap, then these quantities are advanced by the equations

$$x_{n+1} = x_n + v_{\rho n+1}\ (L/v_z), \tag{20}$$

$$v_{\rho n+1} = v_{\rho n} + \delta v_{\rho 0}\ \left(\frac{FRAC\ (x_n/\Delta r) - \Delta r/2}{\Delta r}\right).$$

Here $FRAC$ indicates the fractional part of the expression. Using the dimensionless variables $X_n = x_n/\Delta r$, and $V_{\rho n} = v_{\rho n}/v_z$, the equations can be recast as

$$X_{n+1} = X_n + \gamma V_{\rho n+1}, \tag{21}$$

$$V_{\rho n+1} = V_{\rho n} + \beta[FRAC\ (X_n) - \tfrac{1}{2}],$$

where $\gamma = (L/\Delta r)$ and $\beta = \delta v_0/v_z$. These equations can be easily solved numerically. Typical solutions are shown in Fig. 13. The parameter γ has been taken equal to 20. Using Eq. (19), it can be shown that the parameter β scales as $\beta \sim [1/\gamma\ (f_r/f_z)]^2$. Thus low values of β better fulfill the validity conditions for the equivalent-potential models. In

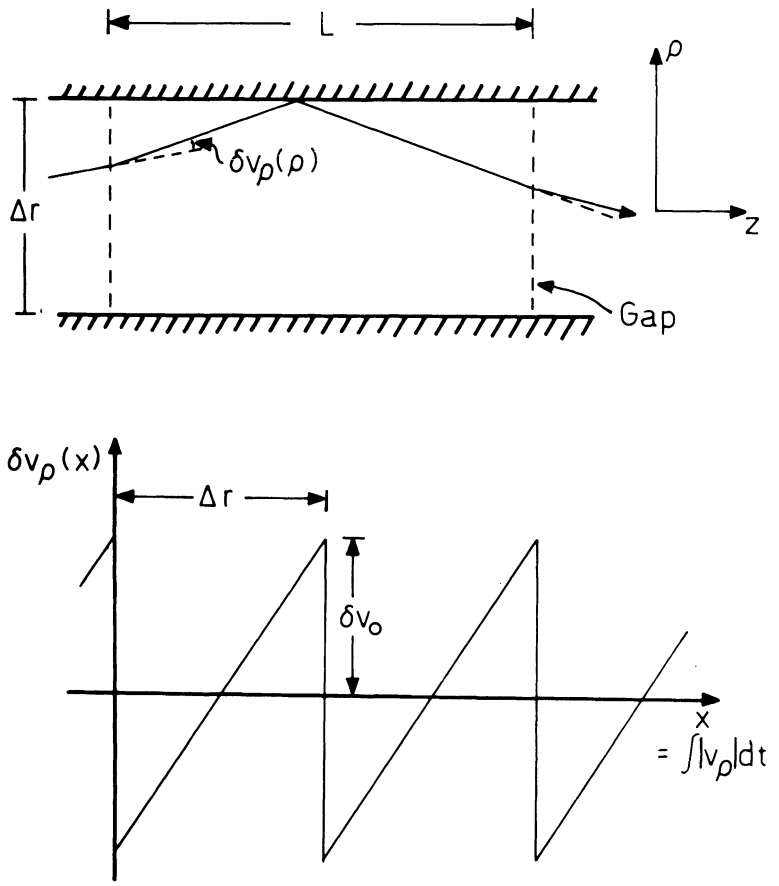

FIGURE 12 a) Simplified geometric model for calculation of ion orbits. Reflections from inner and outer sheaths with instantaneous space-charge deflections at the accelerating gaps. b) Form for computing acceleration gap deflections using the variable x that allows neglect of sheath reflections.

the runs shown, the particle has been started at $\rho = 0$, with an initial velocity $v_{\rho 0}$ chosen so that the effects of the space-charge forces will be strong, but the particle is not trapped on one side of the potential. In the first example [Fig. 13(a)], the choice of parameters makes $f_r \cong f_z/4$. In this case, the effective-potential model conditions are not satisfied. There is little correlation of the deflections, so that they occur in a random manner. The behavior of the transverse velocity is diffusive. The variation following Gap 27 is interesting in that it appears that the deflections have come into resonance with the longitudinal frequency. There is an increase in the average transverse velocity, but the instability rapidly quenches. This is a favorable property of the highly nonlinear confining forces; a change in the transverse velocity caused by a resonance will change the transverse-oscillation frequency to decouple the particle. Resonance effects act mainly to increase the velocity diffusion rate and do not cause exponentiating instabilities. As the parameters are changed to bring the orbits closer to the conditions for the effective potential model ($f_r \ll f_z$), the deflections become more correlated, diffusion effects rapidly decrease, and resonant effects become smaller (because the higher-order resonances would have to act over many radial oscillations to produce a significant change). Effects of increasing f_z/f_r are shown in Fig. 13(b) and (c). In the third case, a well-defined periodic orbit results with a change in the velocity about 0.8 that predicted by the effective-potential model. Thus the model appears to give a good first-order approximation of transverse orbits.

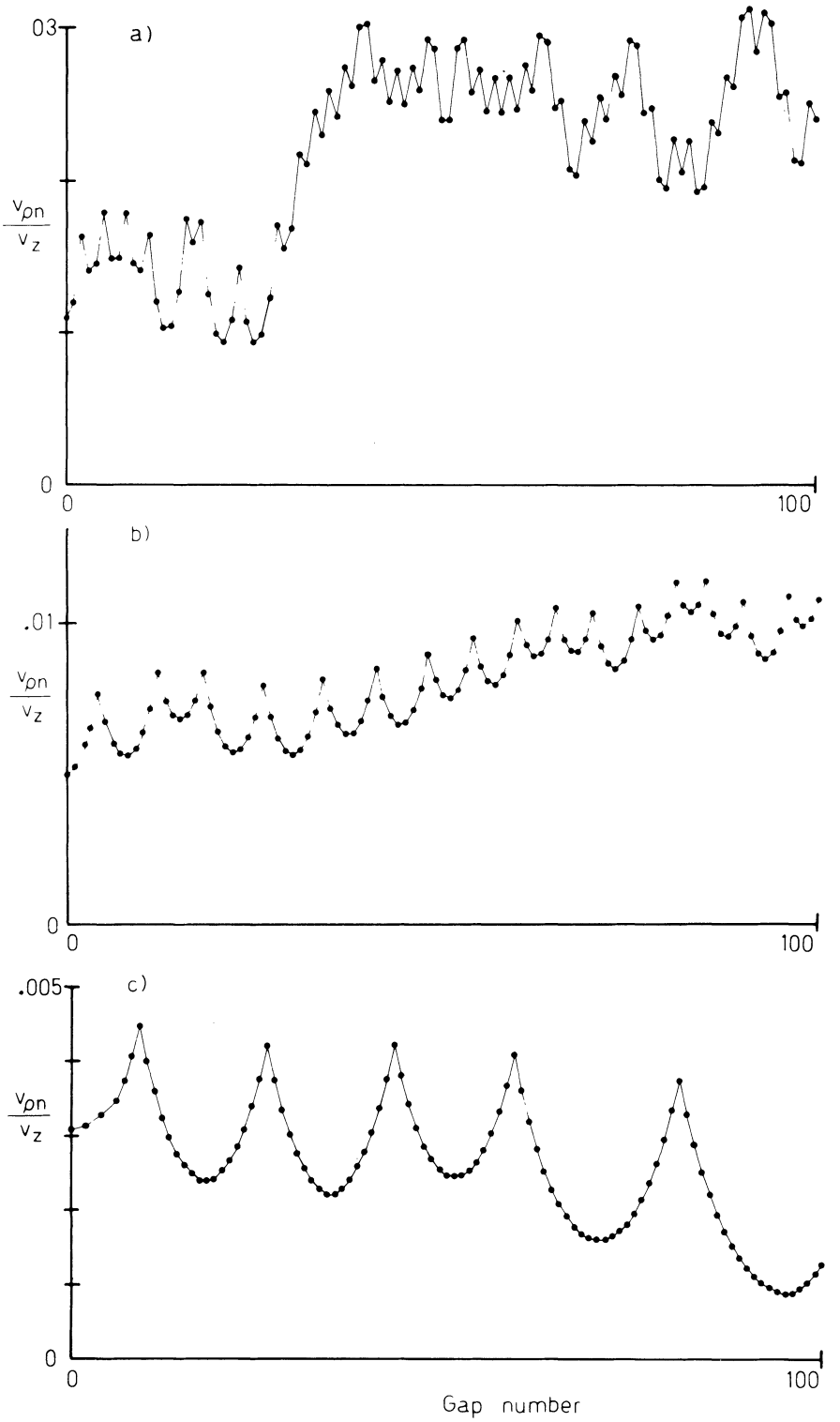

FIGURE 13 Results of particle orbit models. Plots of v_ρ versus gap number. Particles initiated with $X = 0.5$ ($p = 0$) at 0. a) $\gamma = 20$, $\beta = 0.01$, $V_{\rho 0} = 0.01$, b) $\gamma = 20$, $\beta = 0.0025$, $v_{\rho_0} = 0.005$, c) $\gamma = 20$, $\beta = 0.001$, $v_{\rho_0} = 0.0031$.

VII. PRACTICAL ASPECTS

The electron-annulus geometry may be able to accelerate and transport ion beams of a variety of masses with current levels in the range from amperes to kiloamperes. A number of practical aspects of the configuration that may affect its application will be discussed in this section. One of these is the complication of the simple space-charge neutralization behavior when the ion beam has high (E_B/A). As the ion beam fills a drift tube, electrons from the upstream electron source must flow with the head of the beam; therefore, as discussed in Ref. 8, the beam must assume a potential with respect to the source of at least $E_B(m_e/m_i)$ in order to accelerate the electrons to the beam velocity. For ion-beam fusion parameters ($E_B/A \sim 10$ to 25 MeV), this probably would not be a severe problem, because the electron energy need only be 5 to 10 keV at the end of the accelerator. The beam could be at this potential with respect to the wall, in which case the electrostatic sheath would have to increase somewhat to counteract the additional radial electric field, or the source could be referenced to a negative potential with respect to the rest of the drift tube. In any case, for beams exceeding hundreds of amperes, there is enough positive space-charge density to pull electrons into the beam volume. For low currents or high beam velocities, this may not be the case. In conventional accelerators, the area of applicability of this means of neutralization would possibly be limited to the low-β regime. Computer studies are underway to better understand the electron behavior at an accelerating gap in order to make more definitive statements on these limits.

A second area that may pose problems is that of the stability of the electron annulus. In a macroscopic sense, the ion-electron plasmoid in the drift tube is in a region of minimum magnetic field,[19] so that large-scale deformations would not be expected. On the other hand, microscopic instabilities could be important if they produced electron diffusion, which would increase the size of the electron annulus. This would provide an upper limit to the ion-beam pulse length that could be confined. The instabilities would have to occur very rapidly to affect adversely typical pulsed beams or beam bunches ($\lesssim$ 50 nsec). Current experiments have demonstrated the existence of stable electron clouds over microsecond time scales for field stresses exceeding 200 kV/cm.[20,21]

In order to have a controllable longitudinal acceleration of the beam, it is important that the presence of the neutralizing electrons does not affect the charge state of the ions. In other words, the mean free path for ionization must be greater than the length of the accelerator. An exact determination of the ionization probability would depend on the relative velocities of the ions and electrons. The energy of the electrons with respect to the ion beam will probably be on the order of $E_B\,(m_e/m_i)$, which may vary from hundreds of electron volts to many keV. At any rate, the cross section should be less than 10^{-16} cm^2 for injected ions, and will decrease with energy. Typical beam densities at injection are less than 10^{12} cm^{-3}. Thus, the mean free path for ionization of the injected ion beam is greater than 100 m. This allows sufficient distance to accelerate the beam to a point where the cross-section and density decrease make the probability of ionization negligible.

In conventional accelerators with linear focusing elements and space-charge effects, it is possible to tune the focusing to approximately balance the space-charge forces. In terms of the effective-potential model, the focusing and space-charge potentials have the same shape but opposite polarity, so that a net zero well can be obtained. In such a system, space-charge repulsion does not greatly increase the beam's transverse energy. The confining well need only be deep enough to handle the initial transverse energy. In the electron-annulus geometry, such a balance cannot be obtained because of the nonlinear forces involved. Space-charge effects on the beam transverse energy are inevitable; these effects are minimized through the use of electron neutralization. Even though some increase in the transverse energy is unavoidable, there are benefits to be gained from a nonlinear confinement system. For example, it need not be tuned. The sheaths that are set up adjust automatically to changing beam parameters. There is also the advantage that particles in the nonlinear confining wells may not be subject to orbital instabilities since there is no unique oscillation frequency. Particles leave a resonance with a perturbation by gaining or losing transverse energy.

At the expense of locating electron sources and coils for moderate magnetic fields in appropriate areas on the drift-tube structures, important advantages may be gained. There is the possibility of reducing complex and costly magnetic focusing elements. In addition, there is the fact that large currents, possibly orders of magnitude higher than those set by space-charge limitations, could be accelerated and transported. In the case where beam

quality can be relaxed, extremely high currents are possible using electrostatic confinement of the beam. This may make it possible to build medium energy, very high flux machines for industrial or medical applications.

ACKNOWLEDGEMENTS

We would like to thank G. Yonas for his suggestions, and T. Hayward and members of the Los Alamos Meson Facility Accelerator Technology Group for their critical comments. This work was supported by U.S. DOE.

REFERENCES

1. A. W. Maschke, *IEEE Trans. Nucl. Sci.* **NS-22,** 1825 (1975).
2. R. Martin, *IEEE Trans. Nucl. Sci.* **NS-22,** 1763 (1975).
3. A. Faltens, D. L. Judd, and D. Keefe, *Proceedings of the Second International Topical Conference on High Power Electron and Ion Beam Research and Technology,* edited by J. A. Nation and R. N. Sudan (Laboratory of Plasma Studies, Cornell University, 1977), 57.
4. S. Humphries, Jr., J. W. Poukey, and G. Yonas in *Proceedings of the Third International Conference on Collective Methods of Acceleration.*
5. A. W. Maschke, cited in *Final Report of the ERDA Summer Study of Heavy Ions for Inertial Fusion,* edited by R. O. Bangerter, W. B. Hermannsfeldt, D. L. Judd, and L. Smith (Lawrence Berkeley Laboratory, LBL-5543, 1976).
6. See, for instance, R. G. Wilson and G. R. Brewer, *Ion Beams* (J. Wiley and Sons, New York, 1973), p. 143.
7. See, for instance, P. Dreike, C. Eichenberger, S. Humphries, and R. N. Sudan, *J. Appl. Phys.* **47,** 85 (1976), D. S. Prono, J. M. Creedon, I. Smith, and N. Bergstrom, *J. Appl. Phys.* **46,** 3310 (1975), and C. A. Kapetankos, R. K. Parker, and K. R. Chu, *Appl. Phys. Lett.,* **26,** 284 (1975).
8. S. Humphries, Jr., *Appl. Phys. Lett.,* **32,** 792 (1978).
9. S. Humphries, Jr., *J. Appl. Phys.* **49,** 501 (1978).
10. See, for instance, E. Stuhlinger, *Ion Propulsion for Space Flight* (McGraw-Hill, New York, 1964), p. 232.
11. J. W. Poukey and S. Humphries, Jr., *Appl. Phys. Lett.,* **33,** 122 (1978).
12. S. Humphries, C. Eichenberger, and R. N. Sudan, *J. Appl. Phys.* **48,** 2738 (1977), J. Maenchen, L. Wiley, E. Peleg, D. A. Hammer, S. Humphries, Jr., and R. N. Sudan, LPS 244 (Laboratory of Plasma Studies, Cornell University, 1978).
13. D. J. Hohnson, G. W. Kuswa, R. J. Leeper, S. Humphries, Jr., and G. R. Hadley, IEEE Conference Record-Abstract 78CH1357-3NPS (IEEE, 445 Hoes Lane, Piscataway, New Jersey, 1978), 175.
14. The electron source must supply a current comparable to the ion-beam current. For low and medium current applications, hot-cathode sources should be adequate. For currents in the kiloampere range, dense localized plasmas produced by surface discharges can supply the required electron flux for a pulsed beam with small energy investment.
15. J. Maenchen, *The Propagation and Focusing of an Intense Pulsed Neutral Proton Beam from a New Magnetically Insulated Diode,* Master's Thesis, Department of Applied Physics, Cornell University, 1978.
16. In this paper we will use the transverse angular divergence, rather than the emittance, to characterize the quality of beams in nonlinear transport systems. This quantity is defined as $\Delta\theta_x = \sqrt{v_N^2}/v_z$ in one dimension and $\Delta\theta = \sqrt{v_N^2 + v_y^2}/v_z$ in two dimensions. We will consider only beams of constant cross section (although for adiabatic transitions, the product of the transverse velocity divergence ($v_z\Delta\theta$) and the mean beam dimension is a constant). The perpendicular beam energy is defined as $E_{B\perp} = E_B\Delta\theta^2$, where E_B is the longitudinal energy. The angular divergence can characterize the focal properties of the beam. For instance, if the beam is to be focused at a target over a distance D, the mean radius of the focual spot is $D\Delta\theta$, independent of the transverse dimension of the beam in the paraxial approximation. The major advantages to using the angular divergence in this case is that it is unambiguously defined and gives the minimum focal spot, even for filamented, non-elliptical phase distributions. In a uniform, nonlinear transport system with stable particle orbits, the velocity divergence is conserved, whereas the effective emittance may change, depending on how it is defined.
17. T. J. Orzechowski and G. Bekefi, *Phys. Fluids* **19,** 43 (1976), and G. Bekefi and T. J. Orzechowski, *Phys. Rev. Lett.* **37,** 379 (1976).
18. Related calculations are reviewed in J. W. Shearer, Lawrence Livermore Internal Report UCRL-52129, 1976 (unpublished).
19. The geometry discussed in this paper is similar to that of the Polytron, a plasma accelerator. See M. L. Watkins, D. E. Potter, J. D. Kilkenny, M. G. Haines, and A. E. Dangor in *Plasma Physics and Controlled Nuclear Fusion Research* (I.A.E.A., Vienna, 1971), 621.
20. R. E. Kribel, S. C. Luckhardt, and H. H. Fleischmann, Bull. Am. Phys. Soc. **22,** 1130 (1977).
21. S. Humphries, Jr. and G. W. Kuswa, accepted for publication, *Appl. Phys. Lett.*